Auto-Tuning Control of a Switched-Mode Power Converter for Tailored Pulse-Shape Biased Plasma Etching Applications

DOI:
10.1109/ECCE47101.2021.9595672

Document status and date:
Published: 16/11/2021

Document Version:
Accepted manuscript including changes made at the peer-review stage

Auto-Tuning Control of a Switched-Mode Power Converter for Tailored Pulse-Shape Biased Plasma Etching Applications

Qihao Yu, Erik Lemmen, Korneel Wijnands, Bas Vermulst
Department of Electrical Engineering
Eindhoven University of Technology
Eindhoven, the Netherlands
https://orcid.org/0000-0001-5318-434X

***Abstract*—For reaching a high selectivity in plasma etching, it is required to precisely control the plasma ion energy. This can be realized by applying a tailored pulse-shaped voltage waveform to bias the reactor table. The bias waveform is divided into an etching phase and discharge phase, based on the status of the plasma reactor. During the etching phase, the waveform is a negative voltage slope while during the discharge phase, the waveform is a short positive voltage pulse. Recent research has shown that switched-mode power converters can be used to generate this kind of bias waveform. To obtain a narrow ion energy distribution, the voltage slope rate during the etching phase should be accurately tuned.**

Traditionally, the voltage slope rate is tuned manually by finding the optimal ion energy distribution from the measurements by a retarding field energy analyzer. However, measurements using a retarding field energy analyzer is interactive with the plasma thus affecting the etching process. On the other hand, the manual-tuning is inefficient since iterative retuning is required if the operating condition is changed. In this paper, an auto-tuning method is proposed, which enables the power converter to generate the optimal waveform automatically. The control method is fully based on the measurements of voltage and current waveforms on the converter side. Therefore, it is nonintrusive and does not interact with the plasma etching process.

***Index Terms*—Auto-tuning, ion energy, plasma etching, switched-mode power converter**

I. Introduction

Plasma consists of positive ions, negative electrons and neutral particles with an approximately neutral net charge [1]. Plasma is crucial in semiconductor manufacturing, where plasma etching and deposition are used to manipulate the silicon wafer. Fig. 1 shows a schematic representation of a typical inductively coupled plasma (ICP) etching reactor. In the etching process, the target surface material of the substrate wafer on the table is removed by chemical reactions or physical sputtering.

As shown in Fig. 1, while gas is infused from the top, the plasma is ignited and sustained in the chamber by utilizing the electrical breakdown of a neutral gas with the external radio-frequency (RF) power supply through a matching network [2].

The authors gratefully acknowledge the financial support of Prodrive Technologies B.V. and the assistance from Javier Escandon-Lopez, Erik Heijdra, Koen Buskes, Dr. Tahsin Faraz, Yuri Verstappen and Dr. Adrie Mackus.

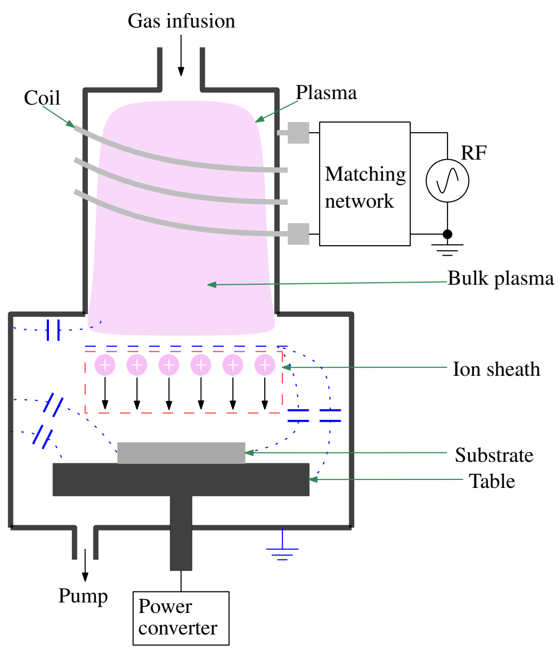

Fig. 1: A typical setup of an inductively coupled plasma chamber.

A power converter is connected to the table, which generates a negative bias voltage on the substrate surface. As a result, the ions in the bulk plasma are attracted and bombard the substrate surface, thus providing extra energy for the chemical reaction or introducing physical sputtering on the substrate surface for material removal.

High-selectivity etching demands efficient removal of the target material while maintaining the other materials, including the etching resist and underlying materials. During etching, the plasma ions should be accelerated to a certain energy, so that they can provide sufficient energy to the substrate surface reactions. Ions with an energy level below the threshold cannot trigger etching or cause a slow reaction rate while ions with too high energy can remove the material that should be retained, thus degrading the selectivity. In general, the ion energy should therefore fall into a specific narrow window. In other words, a narrow ion energy distribution (IED) is desired. Ion energy can

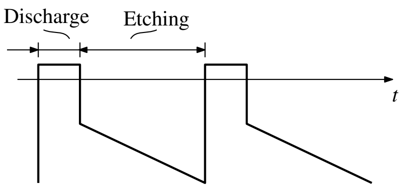

Fig. 2: The tailored pulse-shaped voltage waveform.

be controlled by biasing the substrate surface voltage potential with a power converter [3]–[5]. Different bias voltage waveforms have been studied, including the RF sinusoidal voltage waveform [6]–[9], pulse-shape voltage waveform [10]–[12], and tailored pulse-shaped voltage waveform [13]–[17]. For a typical dielectric substrate, the so-called tailored pulse-shaped voltage waveform has proven to be effective and promising [14], [17]. As depicted in Fig. 2, the tailored pulse-shaped voltage waveform contains a negative voltage slope during the etching phase and a positive voltage pulse during the discharge phase. The negative voltage slope is used to compensate the ion charge effect to achieve a quasi-constant voltage potential on the substrate surface, thus obtaining a narrow IED. The voltage pulse is used to swiftly discharge the substrate.

Switched-mode power converters (SMPC) can be used to generate this waveform [18]. Under a fixed operating condition, there is an optimal voltage slope rate in the etching phase to obtain the narrowest IED. Traditionally, to find the optimal value, voltage slope rates are tuned manually based on IED measurements with a retarding field energy analyzer (RFEA). With iterative manual-tuning, the narrowest IED can be found and the corresponding voltage slope rate is found to be optimal. However, this manual-tuning method suffers from two major drawbacks in industrial applications. On the one hand, the retarding field energy analyzer has to be placed on the top of the substrate wafer during etching, which is interactive with the plasma thus affecting the etching process. On the other hand, the operating conditions, including the plasma power, plasma species, substrate wafer, and so on, could be variant from process to process. As a result, the manual-tuning method has to be conducted repetitively in order to tune the correct slope rate under different operating conditions, which is inefficient.

In this research, an auto-tuning control method is proposed, with which the power converter is able to deliver the optimal bias waveform automatically under different operating conditions. The proposed method advantageously omits the RFEA, with only the measurements of voltage and current waveforms on the converter side required.

II. Auto-tuning control method

Fig. 3 depicts the equivalent electric circuit (EEC) model of the plasma reactor, which is a simplification of the plasma reactor model introduced in [19]. The substrate wafer is placed on the conductive table and the table is connected to the power converter. Usually the substrate material, such as a silicon dioxide wafer, is dielectric, so it can be modelled as a capacitor

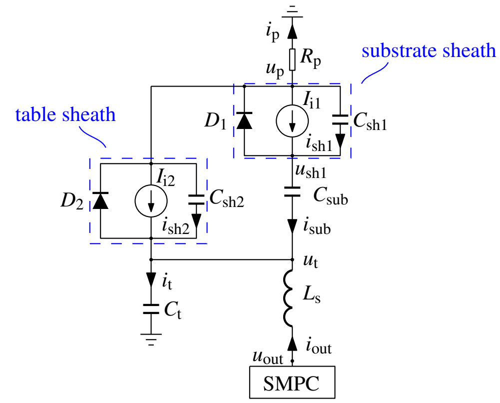

Fig. 3: The equivalent electric circuit model of the plasma reactor system.

C_{sub}. A plasma sheath is formed between the bulk plasma and the substrate surface, the bulk plasma and the table, being the substrate sheath and the table sheath, respectively, as shown in Fig. 3. Plasma sheath is a region where the ion density is larger than the electron density and ions are attracted to the material surface. In the EEC model, each of the sheath is composed of a dc current source, a sheath capacitance, and a diode in parallel. I_{i1} and I_{i2} are the equivalent currents generated by the bombarding ions going to the substrate and the table, respectively, which can be regarded as constant under a fixed plasma condition. C_{sh1} and C_{sh2} are the sheath capacitances. C_{t} is the parasitic capacitance formed between the table and the reactor wall and L_{s} is the stray inductance in the loop. R_{p} is the equivalent plasma resistor. More details on the plasma sheath and the derivation of the EEC model can be found in [19]. Since they are not the focus of this paper, they are skipped here for brevity.

The plasma ions are bombarding the substrate surface with an energy governed by

$$E_{\mathrm{i}} = e\left(u_{\mathrm{p}} - u_{\mathrm{sh1}}\right) \tag{1}$$

where u_{p} is the floating potential of the plasma and can be assumed to be zero here. During etching, the plasma ions should be accelerated to a desired energy. Therefore, the table should be negatively biased and u_{sh1} should be negative. To obtain a narrow IED in high-selectivity etching, u_{sh1} is desired to be quasi-constant. According to the EEC model, u_{sh1} is determined by

$$C_{\mathrm{sub}}\frac{\mathrm{d}\left(u_{\mathrm{sh1}} - u_{\mathrm{t}}\right)}{\mathrm{d}t} = I_{\mathrm{i1}} + C_{\mathrm{sh1}}\frac{\mathrm{d}\left(u_{\mathrm{p}} - u_{\mathrm{sh1}}\right)}{\mathrm{d}t}. \tag{2}$$

By neglecting u_{p}, a constant u_{sh1} leads to

$$\frac{\mathrm{d}u_{\mathrm{t}}}{\mathrm{d}t} = -\frac{I_{\mathrm{i1}}}{C_{\mathrm{sub}}}. \tag{3}$$

In other words, the table voltage u_{t} should linearly decrease with a voltage slope rate of $-\frac{I_{\mathrm{i1}}}{C_{\mathrm{sub}}}$ during the etching phase to exactly compensate the ion charge accumulation on the substrate surface for a constant ion energy [20]. In this paper, this operating condition is defined as the optimal operating point.

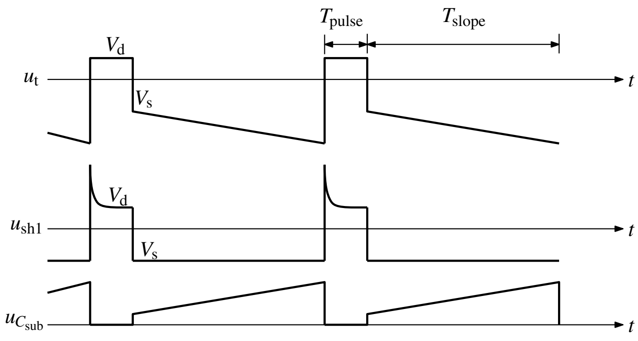

Fig. 4: The typical waveforms of u_{t}, u_{sh1} and $u_{C_{\mathrm{sub}}}$.

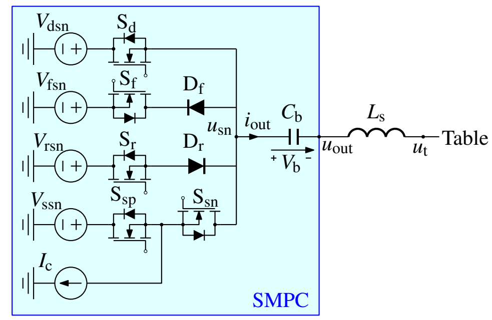

Fig. 5: The topology of the switched-mode power converter.

For a linearly decreasing u_{t} during the etching phase, the plasma etching reactor can be generalized by

$$i_{\mathrm{out}} = \left(\frac{C_{\mathrm{sh1}}C_{\mathrm{sub}}}{C_{\mathrm{sh1}}+C_{\mathrm{sub}}} + C_{\mathrm{sh2}} + C_{\mathrm{t}}\right)\frac{\mathrm{d}u_{\mathrm{t}}}{\mathrm{d}t} - \frac{C_{\mathrm{sub}}}{C_{\mathrm{sub}}+C_{\mathrm{sh1}}}I_{\mathrm{i1}} - I_{\mathrm{i2}}. \quad (4)$$

In this model, all capacitances and currents are assumed to be constant within a reasonable range around the optimal operating point. Therefore, a linearly decreasing u_{t} leads to a dc output current. u_{t} can then be approximated by u_{out} despite the existence of L_{s}.

Because C_{sub} is continuously charging during the etching phase, it is required to discharge it periodically to avoid over-voltage on the substrate. By applying a positive discharge voltage V_{d} to the table, both the substrate and table sheath are restructured and reformed. The capacitor C_{sh1}, C_{sh2} and C_{sub} are discharged through R_{p} in the circuit model. This process is defined by the discharge phase.

The discharge phase should be short to increase the time percentage of the etching process. After C_{sub} is fully discharged, a negative voltage step should be applied to the table to restart the etching phase. The magnitude of this voltage step determines the ion energy at the initial etching phase. Assuming u_{t} changes to a negative value V_{s}, due to the capacitive voltage divider formed by C_{sh1} and C_{sub}, u_{sh1} obtains an initial value governed by

$$u_{\mathrm{sh1}} = \frac{C_{\mathrm{sub}}}{C_{\mathrm{sub}}+C_{\mathrm{sh1}}}V_{\mathrm{s}}. \quad (5)$$

Since C_{sub} is typically much larger than C_{sh1} [19], u_{sh1} can be approximate by V_{s}. Once the etching starts, the bias voltage should linearly decrease with the desired voltage slope rate. As a result, the typical waveforms of the system can be drawn as shown in Fig. 4. The waveform of u_{t} is the so-called tailored pulse-shaped voltage waveform.

To derive the auto-tuning control method, the circuit system generalized by (4) can be further manipulated for simplification. Normally, the value of C_{sh2} and I_{i2} are relatively small and can be neglected [19]. Therefore, a simplified description of the system can be given by

$$i_{\mathrm{out}} = \left(\frac{C_{\mathrm{sh1}}C_{\mathrm{sub}}}{C_{\mathrm{sh1}}+C_{\mathrm{sub}}} + C_{\mathrm{t}}\right)\frac{\mathrm{d}u_{\mathrm{out}}}{\mathrm{d}t} - \frac{C_{\mathrm{sub}}}{C_{\mathrm{sub}}+C_{\mathrm{sh1}}}I_{\mathrm{i1}}. \quad (6)$$

By varying the voltage slope, the dc current changes accordingly. In the optimal operating point governed by (3), (6) can be further simplified as

$$i_{\mathrm{out}} = C_{\mathrm{t}}\frac{\mathrm{d}u_{\mathrm{out}}}{\mathrm{d}t} - I_{\mathrm{i1}}. \quad (7)$$

Since i_{out} is a negative dc value during the etching phase, a positive compensation current $I_{\mathrm{c}} = -i_{\mathrm{out}}$ can be defined for simplicity. Denoting the voltage slope rate by $S = \frac{\mathrm{d}u_{\mathrm{out}}}{\mathrm{d}t}$, the capacitive coefficient $k(S) = -\left(\frac{C_{\mathrm{sh1}}C_{\mathrm{sub}}}{C_{\mathrm{sh1}}+C_{\mathrm{sub}}} + C_{\mathrm{t}}\right)$ and the current coefficient $b(S) = \frac{C_{\mathrm{sub}}}{C_{\mathrm{sub}}+C_{\mathrm{sh1}}}I_{\mathrm{i1}}$, (6) can then be rewritten as

$$I_{\mathrm{c}} = k(S)\cdot S + b(S). \quad (8)$$

Since $C_{\mathrm{t}} \leq \frac{C_{\mathrm{sh1}}C_{\mathrm{sub}}}{C_{\mathrm{sh1}}+C_{\mathrm{sub}}} + C_{\mathrm{t}}$ and $I_{\mathrm{i1}} \geq \frac{C_{\mathrm{sub}}}{C_{\mathrm{sub}}+C_{\mathrm{sh1}}}I_{\mathrm{i1}}$ always stand, when the optimal voltage slope is found, both $k(S)$ and $b(S)$ should theoretically reach their maximum. Therefore, the optimal voltage slope can be found by finding the maximum $k(S)$ and $b(S)$. To find the maximum, a series of different S_n $(n = 1, 2, 3...)$ can be delivered in different output cycles while the corresponding compensation current $I_{\mathrm{c},n}$ is measured. As a result, the corresponding $k(S_n)$ and $b(S_n)$ can be approximated by

$$k(S_n) = \frac{I_{\mathrm{c},n} - I_{\mathrm{c},n-1}}{S_n - S_{n-1}} \quad (9)$$

and

$$b(S_n) = \frac{S_n I_{\mathrm{c},n-1} - S_{n-1}I_{\mathrm{c},n}}{S_n - S_{n-1}}, \quad (10)$$

respectively. The step value of $S_n - S_{n-1}$ should be sufficiently small so that the approximations of (10) and (10) hold. When $k(S_n)$ reaches its maximum value at $S_n = S_m$, the optimal output voltage slope is found to be S_m.

III. Switched-Mode Power Converter

An SMPC was designed and applied to deliver the tailored pulse-shaped voltage waveform with a controlled voltage slope, the topology of which is shown in Fig. 5. The power converter consists of four controllable dc voltage levels V_{dsn}, V_{fsn}, V_{rsn} and V_{ssn} and a controllable dc current source I_{c}. V_{dsn} and V_{ssn} are utilized to generate V_{d} and V_{s} at the output, respectively. Since the reactor is a capacitive load, the stray inductor L_{s} is utilized to resonantly charge and discharge the load capacitor with the dc voltage sources. V_{fsn} and V_{rsn} are

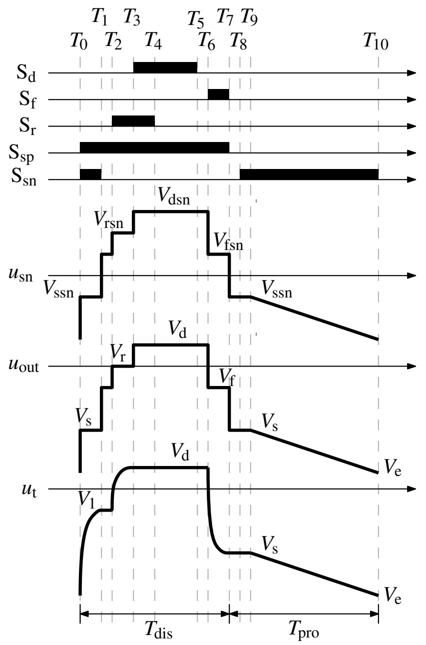

Fig. 6: The operation of the switched-mode power converter.

two intermediate voltage levels used to reduce the resonance during charge and discharge, respectively. The dc current source I_c is realized by an inductor in series with a voltage source. During the etching phase, $i_\mathrm{out} = -I_\mathrm{c}$.

A blocking capacitor C_b is used at the switch-node in order to produce an equal current flowing into both sides of the converter [21]. A self-biasing dc offset voltage V_b is then formed over C_b, the value of which is determined by the plasma condition and the output waveform. The value of C_b should be much larger than C_t and C_sub such that V_b can be assumed constant during steady state operation. In this case, the voltage level V_d, V_r, V_f and V_s of u_t are governed by

$$\begin{pmatrix} V_\mathrm{d} \\ V_\mathrm{r} \\ V_\mathrm{f} \\ V_\mathrm{s} \end{pmatrix} = \begin{pmatrix} V_\mathrm{dsn} \\ V_\mathrm{rsn} \\ V_\mathrm{fsn} \\ V_\mathrm{ssn} \end{pmatrix} - \begin{pmatrix} V_\mathrm{b} \\ V_\mathrm{b} \\ V_\mathrm{b} \\ V_\mathrm{b} \end{pmatrix}. \tag{11}$$

The operation of the converter is described by Fig. 6. A more concrete description of the converter is provided in [18], [22].

IV. Experimental verification

To verify the proposed auto-tuning control method, experiments were conducted with an Oxford Instruments FlexAL plasma reactor, which is a tool for atomic layer deposition but can also used for atomic layer etching, as shown in Fig. 7. The pre-installed RF bias generator was uninstalled and the aforementioned SMPC was used to deliver the required tailored pulse-shaped voltage waveforms. The voltage waveforms were measured by a differential voltage probe and the slope rate were obtained by linear regression from the measurement results. The blocking capacitor of the SMPC was 2 μF. Argon plasma was excited and sustained with an inductively coupled

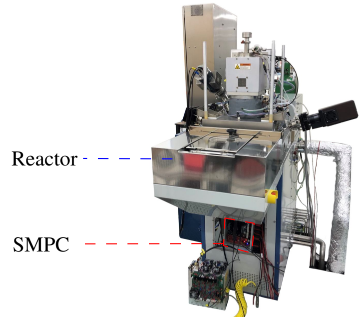

Fig. 7: The FlexAL plasma reactor.

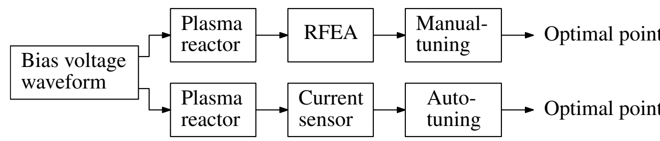

Fig. 8: The experimental verification process.

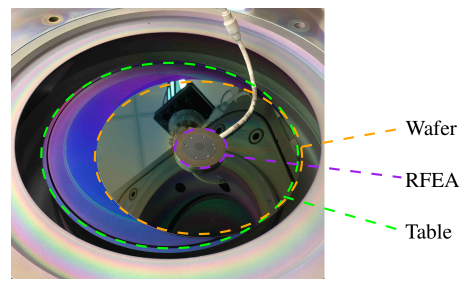

Fig. 9: The reactor table, wafer and RFEA.

RF power of 200 W and the pressure inside the reactor was kept at 2.2 mTorr. An eight-inch silicon dioxide wafer was used as the dielectric substrate.

The experimental verification process is shown in Fig. 8. First, the optimal operating point was found by manual-tuning method with the measurements of the RFEA. The RFEA was placed on the top of the substrate wafer, as shown in Fig. 9. The measurement results of RFEA were recorded by the computer in real-time. By comparing the corresponding IED at various voltage slopes, the optimal operating point can be found. After, the RFEA was removed and the voltage slopes in the similar range were applied while measuring the resultant current waveforms. Consequently, the optimal operating point could be derived based on the proposed auto-tuning control, which could be compared to the manual-tuning result for verification.

Measurement results of a typical manual-tuning are plot in Fig. 10. As can be seen, during the etching phase, when the voltage is linearly decreasing, the output current is dc. Besides, since the load is capacitive, the output current is negative during the etching phase. When varying the voltage slope, the width of IED varies as well. Among the cases shown in Fig. 10, the voltage slope of T3 generates the narrowest IED. Additionally, a narrower IED corresponds to a higher IED peak. As a result, the IED peak can be a quantitative merit

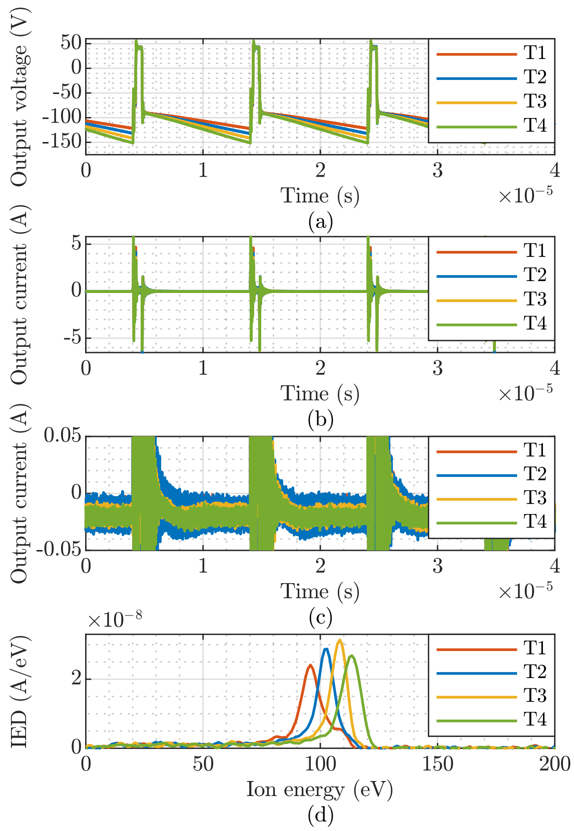

Fig. 10: The measured waveforms of (a) the output voltage, (b) output current, (c) a zoom-in view of the output current, and (d) the corresponding IED measured with RFEA. T1, T2, T3 and T4 indicate different voltage slope rates.

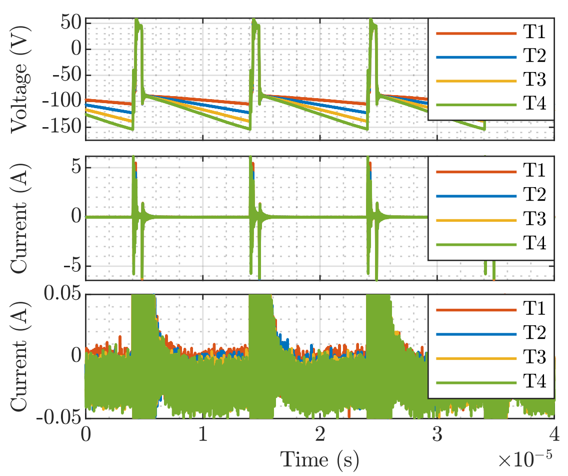

Fig. 11: The measured waveforms, being from top to bottom: bias voltage, output current and a zoomed-in view of the output current, respectively. T1, T2, T3 and T4 indicate different voltage slopes.

used for further comparison.

The bias waveforms in the similar magnitude range were applied to the reactor after the RFEA was removed. The measurement results are shown in Fig. 11. As can be seen,

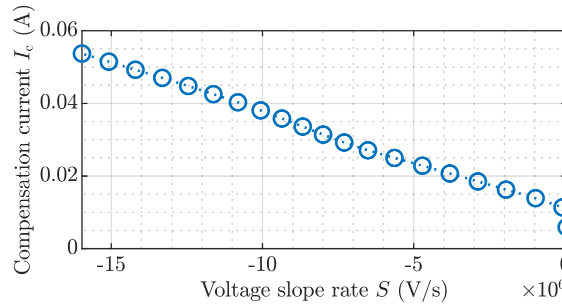

Fig. 12: The measured dataset of S_n and $I_{c,n}$.

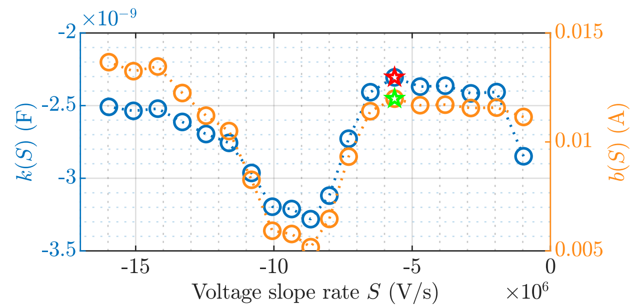

Fig. 13: The relation of $k(S)$ and IED peak versus current I_c.

the electrical response of the plasma reactor is similar to the case with RFEA. However, it should be noted that the auto-tuning method should be conducted without RFEA, since the RFEA interacts the circuit by adding extra parasitic capacitances. Fig. 12 depicts the resultant I_c at different voltage slopes S. As can be seen, it follows a linear relation in general, which matches with (8). Each voltage slope S_n results in a unique compensation current I_c. Furthermore, the corresponding $k(S_n)$ and $b(S_n)$ at different voltage slope S_n can be calculated according to (9) and (10), as shown in Fig. 13. As can be seen, $k(S_n)$ reaches maximum when $S = -5.64 \times 10^6$ V/s as denoted by the red pentagon, while $b(S_n)$ only reaches its local maximum as denoted by the green pentagon. The reason is that I_{i1} is not a strictly constant value in practice. Instead, it increases with an increasing voltage slope S generally, yielding to a larger $b(S_n)$ at a more negative S. Therefore, the auto-tuning method should be conducted based on a maximum $k(S)$.

The auto-tuning method indicates the optimal operating point is at $S = -5.64 \times 10^6$ V/s. The IED peak measured by RFEA is also plotted in Fig. 14 as a comparison, which reaches maximum when $S = -5.96 \times 10^6$ V/s. The optimal operating points found by the manual-tuning and auto-tuning method are close, underlining effectiveness the proposed control method. The difference between the two values could be caused by the parasitic capacitances introduced by the RFEA but requires further verification. Meanwhile, the neglect of the table sheath in the auto-tuning method could also lead to inaccuracy.

V. Conclusion

The tailored pulse-shaped voltage waveform can be used to precisely control the plasma ion energy in plasma etching

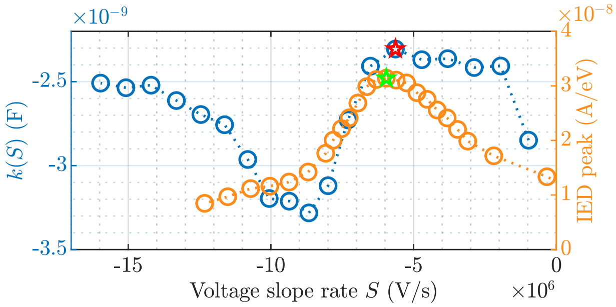

Fig. 14: The relation of $k(S)$ and IED peak versus the voltage slope rate S.

applications. The waveform can be generated by switched-mode power converters. To obtain a narrow ion energy distribution, traditional methods use manual-tuning to find the optimal waveform with the help of an RFEA. In this research, an auto-tuning control method to automatically find the optimal waveform is proposed. The method requires only the measurement of voltage and current waveforms on the converter side while omits the use of RFEA. Experiments have been conducted on a plasma etching reactor for verification. The optimal operating point found by the manual-tuning and auto-tuning is close, which demonstrate the correctness of the proposed method. The proposed auto-tuning control method has been patented [23].

The proposed control method is realized offline in this paper. Therefore, an online realisation is desired in the future. Further research could focus on the verification of the auto-tuning method by using methods other than RFEA, such as etching a material with specific ion energy threshold, to exclude the parasitics introduced by the RFEA.

References

[1] M. A. Lieberman and A. J. Lichtenberg, *Principle of plasma discharges and materials processing*, 2nd ed. John Wiley & Sons, Inc., 2005, no. 1.

[2] N. Matsubara, *Dry Etching Technology for Devices of Compound Semiconductor*, 1st ed. Springer, 2015.

[3] S. Rauf, "Effect of bias voltage waveform on ion energy distribution," *J. Appl. Phys.*, vol. 87, no. 11, pp. 7647–7651, 2000.

[4] X. V. Qin, Y. H. Ting, and A. E. Wendt, "Tailored ion energy distributions at an rf-biased plasma electrode," *Plasma Sources Sci. Technol.*, vol. 19, no. 6, 2010.

[5] D. J. Economou, "Tailored ion energy distributions on plasma electrodes," *J. Vac. Sci. Technol. A Vacuum, Surfaces, Film.*, vol. 31, no. 5, p. 050823, Sep. 2013.

[6] A. Agarwal and M. J. Kushner, "Effect of nonsinusoidal bias waveforms on ion energy distributions and fluorocarbon plasma etch selectivity," *J. Vac. Sci. Technol. A Vacuum, Surfaces, Film.*, vol. 23, no. 5, pp. 1440–1449, Sep. 2005.

[7] D. Zhenfeng, H. Weigang, and W. Younian, "The tuned substrate self-bias in a radio-frequency inductively coupled plasma," *Plasma Sci. Technol.*, vol. 6, no. 6, pp. 2549–2558, 2006.

[8] H. B. Profijt, M. C. M. van de Sanden, and W. M. M. Kessels, "Substrate-biasing during plasma-assisted atomic layer deposition to tailor metal-oxide thin film growth," *J. Vac. Sci. Technol. A Vacuum, Surfaces, Film.*, vol. 31, no. 1, p. 01A106, Jan. 2013.

[9] F. Krüger, S. Wilczek, T. Mussenbrock, and J. Schulze, "Voltage waveform tailoring in radio frequency plasmas for surface charge neutralization inside etch trenches," *Plasma Sources Sci. Technol.*, vol. 28, no. 7, 2019.

[10] E. V. Barnat and T. M. Lu, "Measured energy distributions of ions driven by an asymmetrically pulsed bias during magnetron sputtering," *J. Appl. Phys.*, vol. 92, no. 6, pp. 2984–2989, Sep. 2002.

[11] H. Shin, W. Zhu, L. Xu, V. M. Donnelly, and D. J. Economou, "Control of ion energy distributions using a pulsed plasma with synchronous bias on a boundary electrode," *Plasma Sources Sci. Technol.*, vol. 20, no. 5, 2011.

[12] A. Ui, H. Hayashi, I. Sakai, T. Kaminatsui, T. Ohiwa, K. Yamamoto, and K. Kikutani, "Ion energy control in reactive ion etching using 1-mhz pulsed-dc square-wave-superimposed 100-mhz rf capacitively coupled plasma," *J. Vac. Sci. Technol. A Vacuum, Surfaces, Film.*, vol. 34, no. 3, p. 031301, 2016.

[13] S.-B. Wang and A. E. Wendt, "Control of ion energy distribution at substrates during plasma processing," *J. Appl. Phys.*, vol. 88, no. 2, pp. 643–646, Jul. 2000.

[14] P. Kudlacek, R. F. Rumphorst, and M. C. M. van de Sanden, "Accurate control of ion bombardment in remote plasmas using pulse-shaped biasing," *J. Appl. Phys.*, vol. 106, no. 7, p. 073303, Oct. 2009.

[15] I. T. Martin, M. A. Wank, M. A. Blauw, R. A. C. M. M. van Swaaij, W. M. M. Kessels, and M. C. M. van de Sanden, "The effect of low frequency pulse-shaped substrate bias on the remote plasma deposition of a-si : H thin films," *Plasma Sources Sci. Technol.*, vol. 19, no. 1, p. 015012, Jan. 2010.

[16] Z. Liu, Z. Dai, C. He, and Y. Wang, "Effects of tailed pulse-bias on ion energy distributions and charging effects on insulating substrates," *Plasma Sci. Technol.*, vol. 17, no. 7, pp. 560–566, Jul. 2015.

[17] T. Faraz, Y. G. Verstappen, M. A. Verheijen, N. J. Chittock, J. E. Lopez, E. Heijdra, W. J. Van Gennip, W. M. Kessels, and A. J. MacKus, "Precise ion energy control with tailored waveform biasing for atomic scale processing," *J. Appl. Phys.*, vol. 128, no. 21, p. 213301, 2020.

[18] Q. Yu, E. Lemmen, K. Wijnands, and B. Vermulst, "A switched-mode power amplifier for ion energy control in plasma etching," in *2020 22nd Eur. Conf. Power Electron. Appl. (EPE'20 ECCE Eur.).* IEEE, Sep. 2020, pp. P.1–P.8.

[19] Q. Yu, E. Lemmen, C. G. E. Wijnands, and B. Vermulst, "Model and verification of a plasma etching reactor with a switched-mode power converter," in *12th Int. Conf. Electr. Electromechanical Energy Convers. (ECCE Asia 2021).* IEEE, in press.

[20] E. V. Barnat and T.-M. Lu, "Calculated sheath dynamics under the influence of an asymmetrically pulsed dc bias," *Phys. Rev. E*, vol. 66, no. 5, p. 056401, Nov. 2002.

[21] S.-H. Song and M. J. Kushner, "Role of the blocking capacitor in control of ion energy distributions in pulsed capacitively coupled plasmas sustained in ar/cf4/o2," *J. Vac. Sci. Technol. A Vacuum, Surfaces, Film.*, vol. 32, no. 2, p. 021306, Mar. 2014.

[22] A. W. Driessen, "Voltage waveform generator for plasma processing apparatuses," Patent WO2 020 216 741, Oct. 29, 2020.

[23] Q. Yu, E. Lemmen, and B. J. D. Vermulst, "Determining an optimal ion energy for plasma processing of a dielectric substrate," Patent WO2 021 064 110, Apr. 8, 2021.